

Supplementary Information

Temperature Gradient-driven Motion and Assembly of Two-dimensional (2D) Materials on Liquid Surface: A Theoretical Framework and Molecular Dynamics Simulation

Yongshuai Wen¹, Qingchang Liu¹, Yongshou Liu*

Department of Engineering Mechanics, Northwestern Polytechnical University,
Xi'an, 710129, China

¹ These authors contributed equally.

* Corresponding author: yongshouliu@nwpu.edu.cn

1. Process to calculate energy variation ΔE of the water and graphene infinitesimal system

The surface tension on solid-vapor, liquid-vapor and solid-liquid phases is dependent on temperature¹⁻³. So when the graphene infinitesimal moves with a distance of Δx on the water surface with temperature gradient, the variation of water surface tension, graphene surface tension and graphene-water interfacial tension must be considered. Thus the total energy variation of the water and graphene infinitesimal system can be written as

$$\Delta E = (\gamma_L^H + \gamma_{SL}^L + \gamma_S^L - \gamma_L^L - \gamma_{SL}^H - \gamma_S^H) \Delta x dy \quad \text{S* MERGEFORMAT (1)}$$

where the corner marks, L and H , on the upper right represent low and high temperature.

In fact, according to our simulations, the temperature of graphene sheet changes very little when it moves on the water surface with temperature gradient. Fig. S1(a) depicts the temperature of the graphene sheet in two cases, in which symbols represent the temperature in the simulations and lines correspond to fitting curves. The stable temperature of the graphene sheet is noted as T_g . As can be seen from this figure, after the graphene sheet is in contact with the water surface, its temperature rises rapidly and then reaches a stable stage (indicated in the figure). Fig. S1(b) shows the stable temperature of the graphene sheet at different temperature gradients and initial temperatures. It can be seen from this figure that T_g is closely dependent on temperature gradient and initial temperature. Hence, we can assume that during the movement of the graphene sheet, the temperature change is negligible, that is, the surface tension of the graphene sheet and the graphene-water interfacial tension can be considered unchanged. Thereby, the expression of ΔE becomes

$$\Delta E = (\gamma_L^H - \gamma_L^L) \Delta x dy \quad \text{S* MERGEFORMAT (2)}$$

2. Determination of friction coefficient of graphene sheet on water surface

The Green-Kubo (GK) model is used to determine the friction coefficient λ between water and solid surface, and has the following expression in terms of the surface lateral force autocorrelation function at equilibrium⁴

$$\lambda = \frac{1}{2Ak_B T} \int_0^\infty \langle F_{lateral}(t) \cdot F_{lateral}(0) \rangle_{equ} dt \quad \text{SI* MERGEFORMAT (3)}$$

noting A is the contact area, k_B is the Boltzmann constant, T is the temperature, and $F_{lateral}$ is the lateral force exerted on solid surface by liquid molecules. The factor 1/2 comes from the configuration of single-side contact model of the graphene sheet on water surface⁵. Extensive molecular dynamic (MD) simulations are performed to calculate λ , and the computational model is indicated in Fig. S3(a). Periodic boundary conditions are applied to x and y direction. We choose the average of the plateau values as the friction coefficient⁶. Variation of the friction coefficient with temperature under different surface wettability is depicted in Fig. S3(b).

3. Wettability behavior of water droplet on graphene surface

We use 2000 water molecules for MD simulations. The L-J potential is employed to determine interactions between water and graphene, and the specific L-J parameters are noted in the Section 3 in the article. Firstly, NVT ensemble is performed for water at 300 K for 0.5 ns, afterwards, NVE ensemble is performed for 0.5 ns to achieve a stable configuration of water droplet on the graphene surface, as a result, robust calculations of extracting the contact angle are guaranteed. Carbon atoms are fixed during all the simulations. The timestep is 1 fs. With temperature being 300 K, $\epsilon_{CO}=0.0937$ kcal/mole and $\sigma_{CO}=0.319$ nm, the contact angle is 97° , which is consistent with the acceptable range of $95^\circ - 100^\circ$ ⁷. Fig. S4(a) illustrates the model to extract contact angle by fitting the outermost profile of the water droplet. The inset exhibits the side view of the water droplet on the graphene surface at equilibrium when the temperature is 300 K and $\epsilon_{CO}=0.0937$ kcal/mole.

Simulations of water droplet on graphene surface with different ϵ_{CO} and T are performed, and variation of contact angle θ_C with temperature T under different ϵ_{CO} is plotted in Fig. S4(b). With the increase of T , θ_C has no significant change, meaning that the influence of temperature on the contact angle can be ignored in our analysis. While the effect of ϵ_{CO} is significant, under the same temperature, with the increase of ϵ_{CO} , θ_C shows a monotonous decrease. For instance,

when T is 300 K, with ε_{CO} changing from 0.03 kcal/mole to 0.15 kcal/mole, θ_c changes from 160.0° to 44.9° , which corresponds to the variations of surface wettability from superhydrophobicity to high hydrophilicity.

4. Method to define the velocity of graphene sheet

Velocities of graphene sheet are obtained by fitting the theoretical displacement-time curves and the stable sections of the simulated displacement-time curves linearly, as shown in Fig. S8(a) and Fig. S8(b). The magnitude of the velocity equals to the slope of fitted curve, which is indicated in the figure. The detailed method to determine the stable section is illustrated as the following: from the first point to the last point, the authors take each point as the target point, and select a series of points starting from the target point (the time length of these points accounts for 50% of total time length), we call these points point column. Then, the authors fit the point column linearly and take the slope and variance as a set of characteristic parameters. After all the points are handled in this way, the authors change the time length of point column from 50% to 60%, 70%,..., 100%, and the similar way is employed for each point. Finally, all the variances of each point column are compared, and the point column with the lowest variance is taken as the final point column, which is taken as the stable section of the curve.

5. Influence of flexibility of graphene on the driving behavior

The influence of flexibility of graphene sheet on the driving behavior is studied using different layers of graphene (the bending stiffness of three-layers graphene is about four times than the value of monolayer graphene, which means three-layers graphene has low flexibility), and the theoretical and simulated results are plotted in Fig. S9. The stable sections of the theoretical curves of single-layer and three-layers graphene have almost the same slopes, which are 25.3 and 24.2 m/s, respectively. The slopes of the stable sections of the simulation results are 20.4 and 19.1 m/s, respectively, which are also very close. Therefore, we can conclude the flexibility of graphene has negligible influence on the driving behavior. The reasons can be found in our theory, firstly, we assume the graphene sheet stays on the water surface with one

side fully in contact with water. In this case, the solid-liquid interaction will prevent the out-of-plane deformation, because if this happens, there will be gaps between water and graphene, causing the system energy increases. Secondly, the liquid is in static, with no capillary wave or other deformation on the surface, Although there is fluctuation, the whole water surface is relatively flat. As a result, the graphene sheet is always relatively flat (the area of graphene is large enough compared to the local fluctuation of water surface, for example, 7, 9, 11 nm^2 in our simulations) with negligible deformation.

Reference

1. W. V. KAYSER, Temperature Dependence of the Surface Tension of Water in Contact with Its Saturated Vapor, *Journal of Colloid and Interface Science*, 1976, **56**, 622-627.
2. A. R. Nair and S. P. Sathian, A molecular dynamics study to determine the solid-liquid interfacial tension using test area simulation method (TASM), *J Chem Phys*, 2012, **137**, 084702.
3. R. Ramirez and C. P. Herrero, Thermal control of graphene morphology: a signature of its intrinsic surface tension, *Phys. Rev. B*, 2018, **97**, 235426-.
4. L. Bocquet and J. L. Barrat, On the Green-Kubo relationship for the liquid-solid friction coefficient, *J Chem Phys*, 2013, **139**, 044704.
5. Q. Liu and B. Xu, A unified mechanics model of wettability gradient-driven motion of water droplet on solid surfaces, *Extreme Mechanics Letters*, 2016, **9**, 304-309.
6. K. Falk, F. Sedlmeier, L. Joly, R. R. Netz and L. Bocquet, Molecular origin of fast water transport in carbon nanotube membranes: superlubricity versus curvature dependent friction, *Nano Lett*, 2010, **10**, 4067-4073.
7. F. Taherian, V. Marcon, N. F. van der Vegt and F. Leroy, What is the contact angle of water on graphene?, *Langmuir*, 2013, **29**, 1457-1465.
8. X. Chen, L. Zhang, Y. Zhao, X. Wang and C. Ke, Graphene folding on flat substrates, *Journal of Applied Physics*, 2014, **116**.

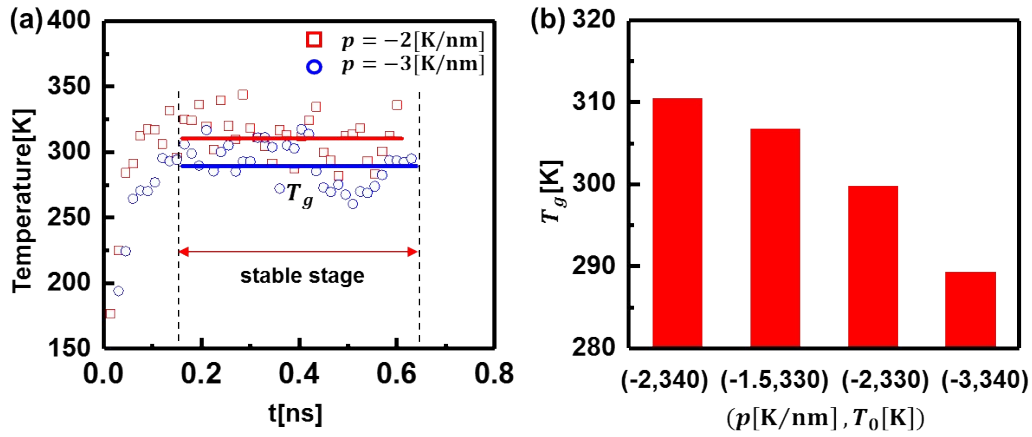


Fig. S1(a) Simulative temperature of the graphene sheet in two cases with different temperature gradients. The contact angle, initial temperature, geometry shape and area of the graphene sheet are set as 97° , 340 K, circle and 9 nm^2 . **(b)** Stable temperature of the graphene sheet under different temperature gradients and initial temperatures. We set the graphene sheet being circle, the area being 9 nm^2 and the contact angle being 97° .

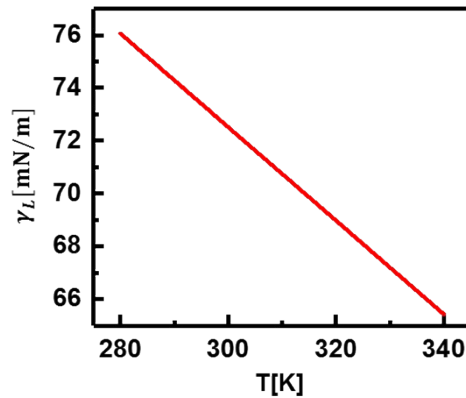


Fig. S2. Variation of the surface tension of water with temperature.

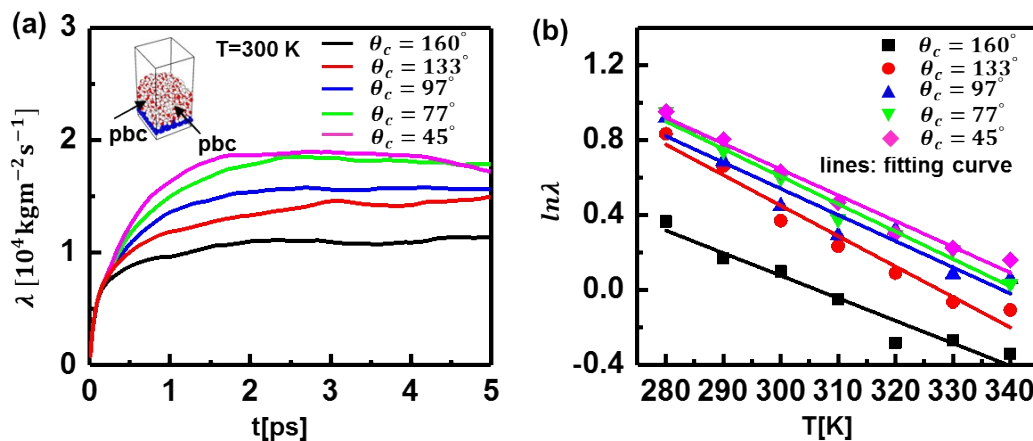


Fig. S3. The process to calculate friction coefficient λ and variation of λ with temperature under different surface wettability. **(a)** Estimation of friction coefficient of water film on a graphene surface with different contact angles when $T = 300 \text{ K}$. The inset shows the MD model. **(b)** Variation of friction coefficient with temperature under different surface wettability represented by θ_c , where markers represent MD simulative results, and lines correspond to fitting results.

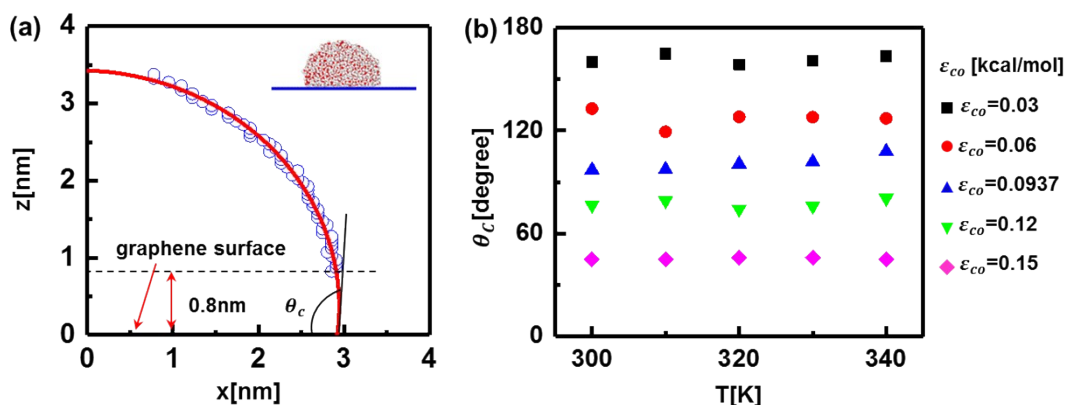


Fig. S4. Model to extract contact angle and variation of contact angle with temperature under different surface wettability. **(a)** Model to extract contact angle by fitting the outermost profile of the water droplet. The blue circles represent the water droplet boundary and the red line corresponds to fitting curve. **(b)** Variation of contact angle with temperature under different surface wettability.

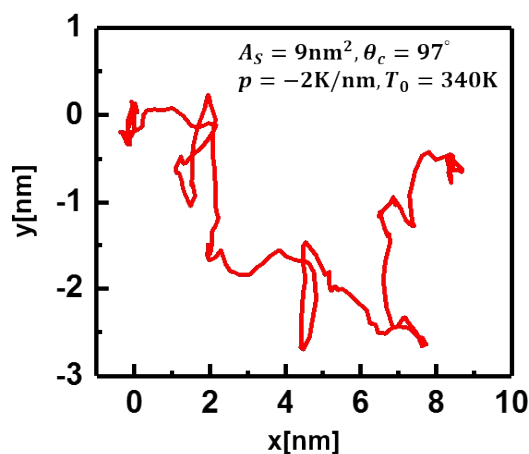


Fig. S5. Actual motion trajectory of graphene sheet on the water surface with temperature gradient on x direction. Random movement exists on the direction perpendicular to the temperature gradient because no gradient exists.

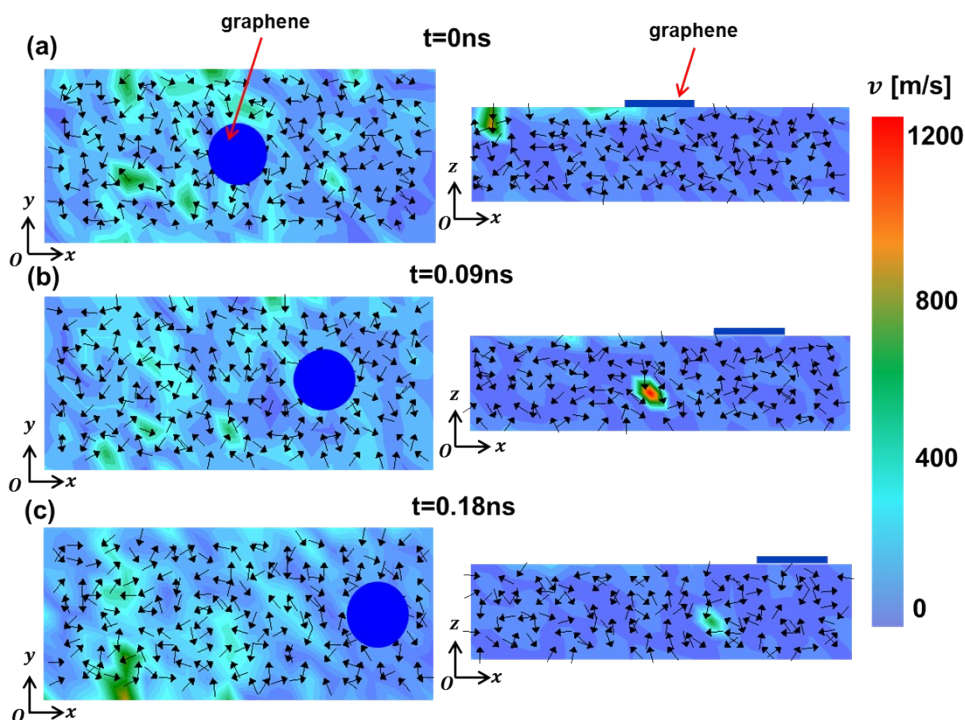


Fig. S6. Velocity fields of water at three time moments when the temperature gradient is -2 K/nm, initial temperature is 340 K, contact angle is 160° and the area of the graphene sheet is 9 nm^2 . **(a)** corresponds to $t=0$ ns, **(b)** corresponds to $t=0.09$ ns and **(c)** corresponds to $t=0.18$ ns.

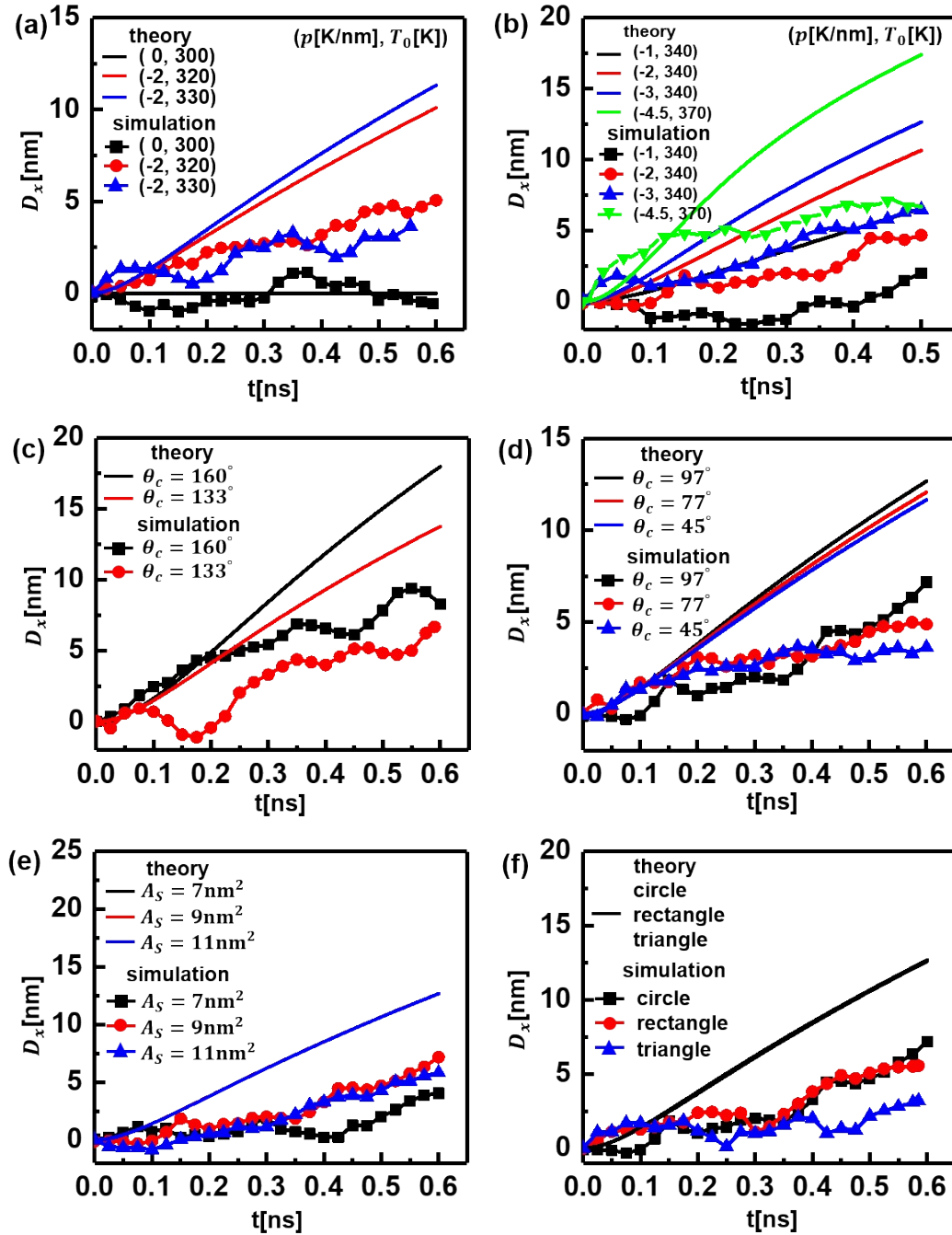


Fig. S7. Theoretical and simulation displacement-time curves of different cases. Lines without markers represent theoretical results and dotted lines represent simulation results. **(a)** The displacement-time curves of three kinds of temperature fields (different p and T_0) when the contact angle is 97° , the area is 9 nm^2 and the shape is circle. **(b)** Other three displacement-time curves of different temperature fields and settings are the same as **(a)**. Setting the temperature gradient being -2 K/nm , initial temperature being 340 K , area being 9 nm^2 and geometry shape being circle, the displacement-time curves under five kinds of surface

wettability are depicted in (c) and (d). (e) Theoretical and simulative displacement-time curves under three area types ($7, 9, 11 \text{ nm}^2$). The temperature gradient, initial temperature, contact angle and geometry shape are set as -2 K/nm , 340 K , 97° and circle. (f) Considering the effect of geometry shape (circle, rectangle and triangle), the displacement-time curves under three types of shape are exhibited when the temperature gradient is -2 K/nm , the initial temperature is 340 K , the contact angle is 97° and the area is 9 nm^2 .

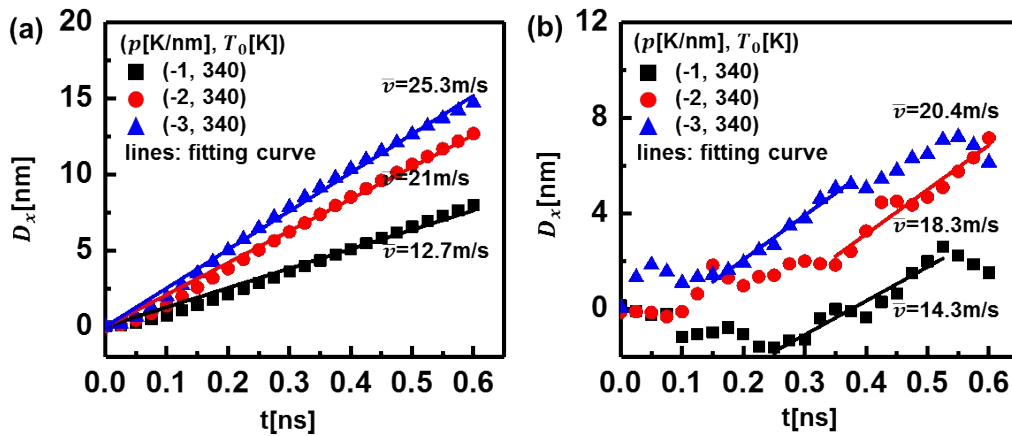


Fig. S8(a) Fitting the theoretical results linearly under three kinds of temperature fields. Lines are fitting curves, and the magnitude of the velocity equals to the slope. Setting the contact angle being 97° , the area being 9 nm^2 and the shape being circle. **(b)** Linearly fitting of the stable sections of the simulative results under the same three kinds of temperature fields. Annotations in this figure and the settings are the same with (a).

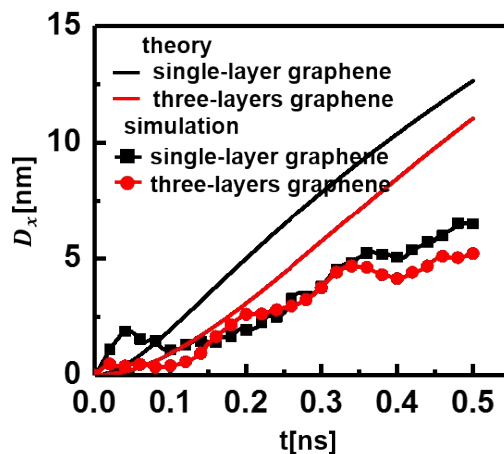


Fig. S9. Theoretical and simulated displacement-time curves of single-layer and three-layers graphene.

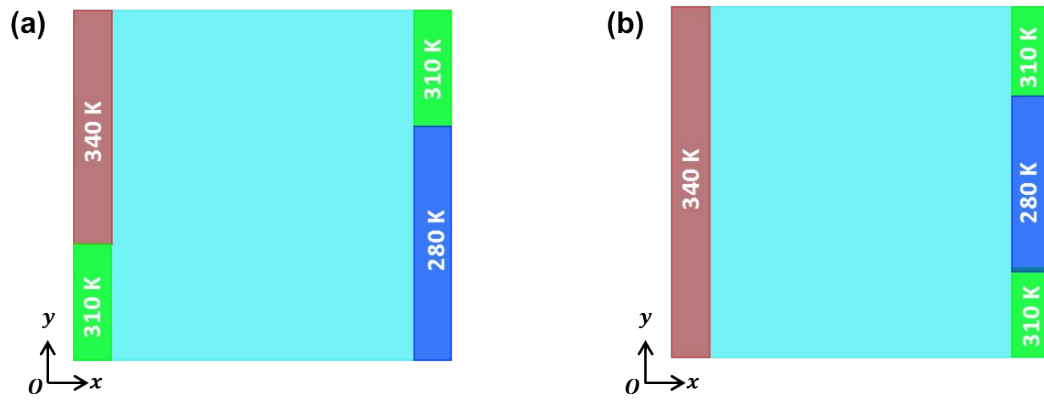


Fig. S10. Schematic illustrations of the arrangement of the temperature field in the directional actuation and assembly parts. **(a)** Illustration of the arrangement of the temperature field with $\alpha = -14.4^\circ$. **(b)** Schematic illustration of the arrangement of the assembly temperature field.

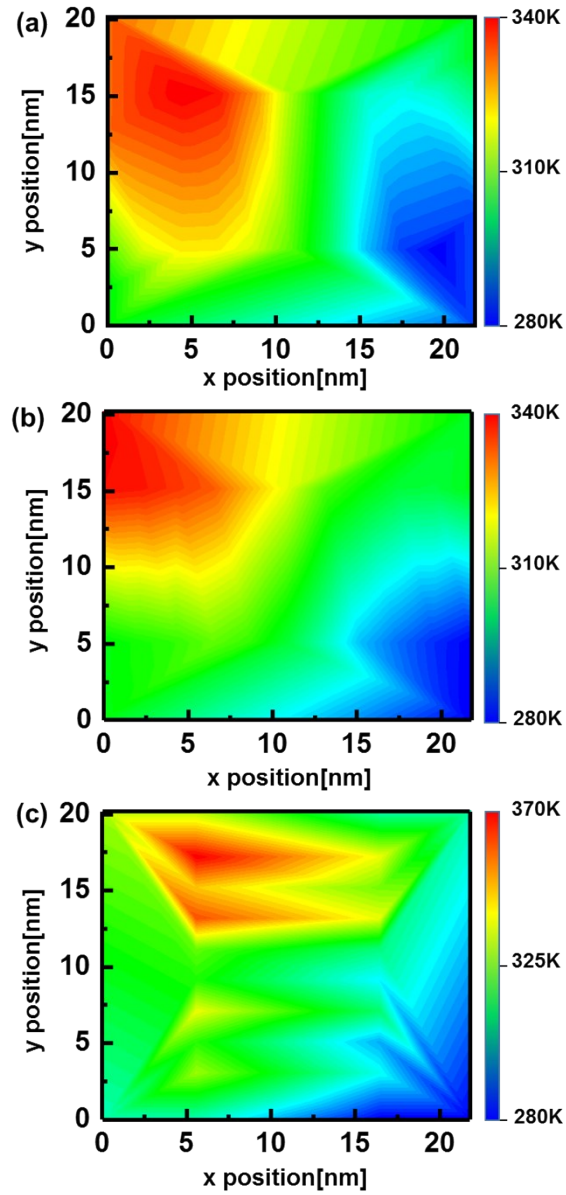


Fig. S11(a) The simulative temperature field with $\alpha = -14.4^\circ$. **(b)** The simulative temperature field with $\alpha = -26.9^\circ$. **(c)** The simulative temperature field with $\alpha = -59.0^\circ$

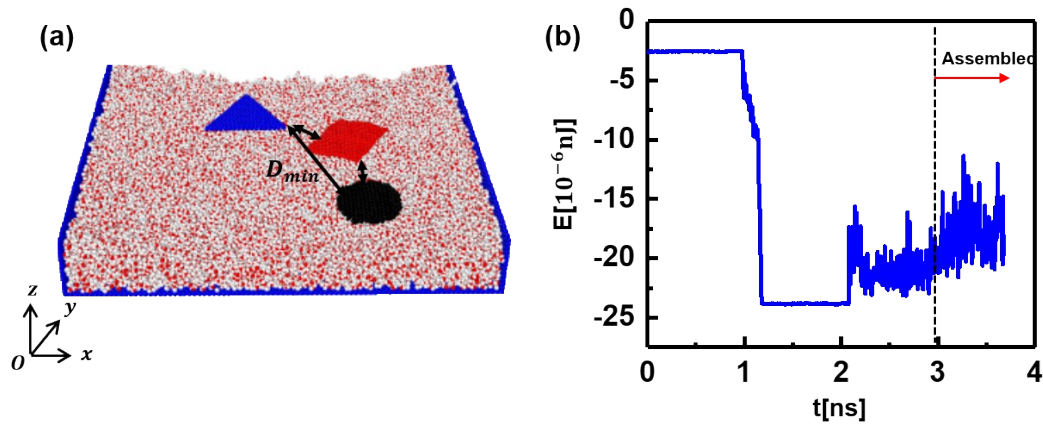


Fig. S12. (a) Schematic illustration of the minimum distance D_{min} between three graphene sheets. (b) Total energy variation during simulation, the assembly process is indicated in the figure.